Virtual Screening, Identification, and Biochemical Characterization of Novel Inhibitors of the Reverse Transcriptase of Human Immunodeficiency Virus Type-1

Alon Herschhorn[†] and Amnon Hizi*

Department of Cell and Developmental Biology, Sackler School of Medicine, Tel Aviv University, Tel Aviv 69978, Israel

Received April 24, 2008

The reverse transcriptase (RT) of human immunodeficiency virus type-1 (HIV-1) is a leading target in current antiretroviral therapy. Unfortunately, drug-resistant RT mutants evolve under the pressure of these drugs, and therefore, new anti-RT inhibitors are constantly required for HIV-1/AIDS treatment. We virtually screened a large chemical library of compounds against two crystal structures of HIV-1 RT to identify novel inhibitors. Top-scoring compounds were tested experimentally; 71 inhibited the RT-associated DNA polymerase, while several also inhibited HIV-1 pseudovirus infection in a cell-based assay. A combination of substituents from two structurally related inhibitors in a single molecule improved the inhibition efficacy. This compound strongly suppressed the RT-associated activity also protecting human lymphocytes from HIV-1 infection. RT inhibition by this compound was reversible and noncompetitive. This molecule and another structurally unrelated potent compound inhibited a known drug-resistant mutant of HIV-1 RT and affected moderately the HIV-2 RT-associated DNA polymerase. These inhibitors may serve as promising anti-HIV lead compounds.

Introduction

The reverse transcriptase (RT)[a] of human immunodeficiency virus type-1 (HIV-1) is a leading target in current therapy treatment for HIV-1 infection.[1−3] RT catalyzes the synthesis of a double-stranded DNA by copying the viral single-stranded genomic (+) RNA in a complex process that requires three distinct RT activities. The first activity is the RNA-dependent DNA polymerase (RDDP) that performs the synthesis of (−) cDNA strand from the viral RNA template. Concomitantly, the RNA strand in the nascent RNA−DNA heteroduplex is hydrolyzed by the ribonuclease H (RNase H) activity of RT. This is followed by DNA-dependent DNA polymerase (DDDP) activity that synthesizes the second DNA strand using the already synthesized cDNA strand as a template. These three interconnected activities generate the provirus DNA that is subsequently integrated into the cellular genomic DNA by the viral enzyme integrase.[4] Since all RT activities are absolutely necessary for completing the viral life cycle, blocking any one of them protects target cells from a productive viral infection.

Non-nucleoside RT inhibitors (NNRTIs) are a variety of hydrophobic noncompetitive inhibitors of HIV-1 RT that are presumed to bind specifically to a hydrophobic pocket located in the proximity of the DNA polymerase active site of RT.[5] Most NNRTIs are highly specific against HIV-1 RT, and therefore, they are usually not toxic to human cells. However, this high specificity also poses a significant obstacle for their systematic use in HIV-1/AIDS patients, due to their reduced efficacy against mutated variants of RT in the infectious HIV-1 population.[6] Consequently, intensive efforts have been directed in recent years to finding novel broad-spectrum NNRTIs that inhibit both wild-type and variant HIV-1 RTs that are resistant to the currently used antiretroviral drugs. This search has recently led to the discovery of several new highly efficient HIV-1 RT inhibitors, including 4-({6-amino-5-bromo-2-[(4-cyanophenyl)amino]-4-pyrimidinyl}oxy)-3,5-dimethylbenzonitrile(TMC-125,etravirine),*N*-[4-(aminosulfonyl)-2-methylphenyl]-2-[4-chloro-2-(3-chloro-5-cyanobenzoyl)phenoxy]acetamide (GW-678248), 5-bromo-*N*-[4-chloro-5-isopropyl-3-methyl-1,3-thiazol-2(3*H*)-ylidene]-2-hydroxybenzenesulfonamide (YM-215389), 4-({4-[(2,4,6-trimethylphenyl)amino]pyrimidin-2-yl}amino)benzenecarbonitrile (TMC-120, dapivirine), and 4-{[4-({4-[(1*E*)-2-cyanoethenyl]-2,6-dimethylphenyl}amino)-2-pyrimidinyl]amino}benzonitrile (R278474, rilpivirine).[7−10] Unfortunately, HIV-1 RT is quite flexible with an outstanding ability to tolerate mutations while remaining functionally active; consequently, new inhibitors are constantly required to increase the available arsenal against HIV and to fight AIDS.

Novel inhibitors against HIV-1 RT are usually identified by either screening a very large number of compounds against the recombinant RT enzyme or testing the compounds for their ability to protect susceptible cells from a productive HIV-1 infection.[11−14] The latter method also requires an additional step for identifying among the active inhibitors those compounds that are specifically directed against HIV-1 RT (while compounds not active against HIV-1 RT may suppress viral infectivity by other mechanisms). Such screenings and the subsequent optimization of the inhibitors by systematic chemical modifications are highly time and resource consuming intensive. Therefore, faster and more efficient strategies that facilitate and shorten the discovery process would be extremely beneficial.

Molecular modeling is one approach that could be used to narrow the number of compounds, found in a chemical library containing an extraordinarily high number of random molecules,

* To whom correspondence should be addressed: Department of Cell and Developmental Biology, Sackler School of Medicine, Tel Aviv University, Tel Aviv 69978, Israel. Telephone: 972-36409974. Fax: 972-36407432. E-mail: ahizy@post.tau.ac.il.

† This work was performed in partial fulfillment of the requirements for a Ph.D. degree from the Sackler School of Medicine.

[a] Abbreviations: RT, reverse transcriptase; HIV-1, human immunodeficiency virus type-1; RDDP, RNA-dependent DNA polymerase; DDDP, DNA-dependent DNA polymerase; RNase H, ribonuclease H; AIDS, acquired immunodeficiency syndrome; NNRTIs, non-nucleoside RT inhibitors; PETT, phenylethylthiazolylthiourea; TSAO, [2′,5′-bis-*O*-(*tert*-butyldimethylsilyl)-3′-spiro-5″-(4″-amino-1″,2″-oxathiole-2″,2″-dioxide)]-β-D-pentofuranosyl; KF, Klenow fragment of *Escherichia coli* DNA polymerase; GFP, green fluorescent protein; VSV, vesicular stomatitis virus; PV, Pseudovirus; TI, therapeutic index.

10.1021/jm800473d CCC: $40.75
Published on Web 08/23/2008

into a smaller list of the potentially effective inhibitors. One of the main tools used in molecular modeling for this purpose is virtual screening. In this technique, each member of a large available chemical database is docked into the active site of an enzyme of interest. The compounds are then ranked according to their potential molecular interactions with the enzyme. Eventually, the top-scoring compounds can be obtained and tested for their capacity to inhibit in vitro the activity of the enzyme. The typical virtual screening approach can be further improved by using more than one crystal structure of the enzyme, as was recently shown by us for inhibitors of HIV-1 RT.[15,16] In this setting, the results retrieved from several structures are integrated and further analyzed before the selection of the final compounds.

In this work, we have extended our previous study to identify novel inhibitors of HIV-1 RT by virtually screening a new commercially available library of compounds (Leadquest3) against two crystal structures of HIV-1 RT. This approach led to initial identification of several potential inhibitors that inhibited the RT-associated DNA polymerase activities and also protected susceptible cells from HIV-1 pseudovirus infection. Moreover, combining functional groups of two related effective compounds resulted in a potent inhibitor that inhibited the RDDP activity of recombinant HIV-1 RT with an IC_{50} value (apparent concentration that inhibits 50% of the initial RT activity) of ~510 nM. This compound also inhibited the infection of human lymphocytes by HIV-1 pseudovirus with an IC_{50} value of ~168 nM.

Results

Virtual Screening of a Chemical Library and Analysis of Potential Inhibitors. We have virtually screened a chemical library of 46000 compounds available in the Tripos Leadquest3 library against two crystal structures of HIV-1 RT, to identify novel inhibitors of HIV-1 RT. The structures of all molecules in the library were energy-minimized and then docked into the NNRTI binding pocket of the heterodimeric (p66/p51) structure of HIV-1 RT using Surflex (see Experimental Section). Two specific RT structures (found in PDB entries 1fk9 and 1dtq) were selected on the basis of the high resolution at which they were determined, and since the RTs in these structures were originally cocrystallized with two of the most potent HIV-1 RT inhibitors. Accordingly, the specific conformation of the hydrophobic pocket in these precise structures is likely to represent the most appropriate inhibitory state of HIV-1 RT. Both structures were used in parallel to account for subtle differences between various RT structures, thus enabling more reliable docking scores. Top-scoring compounds interacting, in silico, with both RT structures with a high affinity were further analyzed by visual inspection of their docked conformation for the quality of the docking process. Consequently, of all the screened library molecules, a total of 740 potential compounds were eventually selected and purchased for further experimental evaluations.

All selected chemicals were tested at a final concentration of 50 μg/mL (average of 156 $\pm$ 23 μM with a range from 105 to 260 μM) for inhibiting in vitro the RDDP activity of recombinant HIV-1 RT, as compared with this activity in the absence of any inhibitor. The RDDP activity was tested first, since it is unique to RTs and distinct from any other DNA polymerases that use DNA as a template. Most compounds exhibited no effect or a weak effect on the RT-associated RDDP activity, while 71 of them (9.6%) inhibited more than 84% of RT activity at the tested concentration (with a range from 84.1 to 99.9%). Of these 71 RT inhibitors, 16 compounds were selected for further evaluation on the basis of their high RT inhibition efficiency and their structural diversity (Table 1), whereas compound **17** was selected later on the basis of its similarity to compound **7**.

Each substance was also tested for its capacity to inhibit the DNA-dependent DNA polymerase activity of RT at the same 50 μg/mL concentration. All tested compounds also inhibited this activity with varying efficiencies that resulted in RT residual activities between 3.1 and 52.3% (Table 1). In general, the inhibition of the DDDP activity observed was slightly less efficient than the inhibition of the RDDP activity, and this may reflect differences in the experimental conditions used to assay each of the enzymatic activities.

The 17 selected inhibitors were further tested for their ability to protect human lymphocytes from HIV-1 pseudovirus infection. In this assay, HIV-1 virions carry a viral mRNA backbone into which the coding sequence for the green fluorescent reporter gene was inserted. The necessary HIV-1-associated proteins are supplied in trans during the packaging step along with the vesicular stomatitis virus (VSV)-G envelope protein, which enables the virions to infect a wide range of cells (see Experimental Section). Productive infection results in the expression of green fluorescent protein (GFP) in the target cells that can be monitored by fluorescent microscopy and quantitatively measured by flow cytometry (see Figure 1). Of the 17 anti-HIV-1 RT inhibitors, seven compounds (41%, or 37.5%, not including compound **17** that was added on the basis of its similarity to compound **7**) also suppressed HIV-1 pseudovirus infection with apparent IC_{50} values between 0.23 and 7.7 μM (Table 1). This finding implied that these compounds could actually penetrate the plasma membrane and inhibit RT activity within the virus-infected cells. Interestingly, compounds **1**, **5**, **9**, **12**, **13**, and **15** share a similar structural backbone with phenylethylthiazolylthiourea (PETT, a known NNRTI) derivatives, containing phenyl, furan, or cyclohexane rings, instead of the pyridine rings found in these original PETT derivatives.[17,18] Due to the similarity of these six compounds, they were not further investigated in this study (although compound **12** inhibited efficiently HIV-1 pseudovirus infection). Accordingly, we have further focused on the other 11 compounds (Table 1). Most of these inhibitors also include thiourea, but they are quite different from any PETT derivatives in having one or three aromatic rings and different substituents on the aromatic groups, with a few of them also including a long and flexible tail.

Structure−Activity Relationships of 1-(3-Propoxypropyl)-thiourea Derivatives. The most potent novel anti-RT inhibitor found in the cell-based pseudovirus assay was *N*-(4-bromo-1*H*-pyrazol-3-yl)-2,1,3-benzothiadiazole-4-sulfonamide (compound **3**, excluding compound **12**, for reasons described above) that inhibited HIV-1 infection with an apparent IC_{50} value of ~374 nM (Table 1). Interestingly, among the other specific anti-HIV-1 RT inhibitors, two compounds, which were unrelated to compound **3**, shared the 1-(3-propoxypropyl)thiourea group (compounds **7** and **17**). They both moderately inhibited HIV-1 infection with apparent IC_{50} values of ~3 μM (Table 1), and therefore, the potential inhibition outcome of this functional group was further explored.

Twenty-three additional derivatives of compounds **7** and **17**, all containing the 1-(3-propoxypropyl)thiourea functional group, were further purchased and then tested for their ability to inhibit the recombinant HIV-1 RT. Some of these compounds were identified from the original Leadquest3 library, whereas others were selected from different databases.

Table 1. Inhibition Profile of Specific Anti HIV-1 RT Inhibitors[a,b,c]

Compound[a]		Residual activity (%) [b]		IC_{50} of HIV-1 PV infection [μM][C]
id	Structure	HIV-1 RT RDDP	HIV-1 RT DDDP	
1	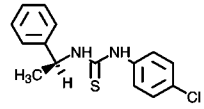	11.4 ± 2.17	21.7 ± 2.0	4.0 ± 0.6
2	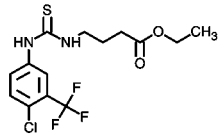	0.7 ± 0.5	8.6 ± 1.8	1.6 ± 0.2
3	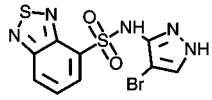	2.2 ± 0.1	13.0 ± 3.4	0.37 ± 0.05
4	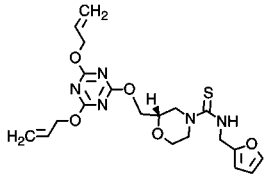	5.6 ± 2.0	22.4 ± 7.9	>20
5	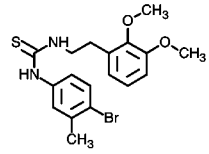	5.1 ± 1.2	15.6 ± 6.4	7.7 ± 1.2
6	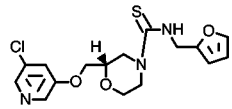	1.1 ± 0.5	7.0 ± 2.0	>20
7	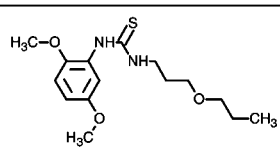	13.2 ± 1.5	28.7 ± 0.5	3.0 ± 0.3
8	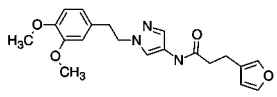	10.9 ± 2.62	26.6 ± 4.8	>20
9	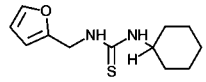	5.2 ± 2.6	10.9 ± 1.6	> 20
10	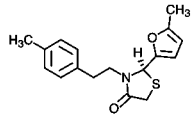	2.0 ± 0.3	3.1 ± 2.0	>20
11	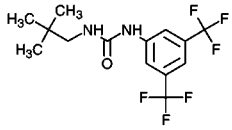	1.7 ± 0.5	7.9 ± 1.8	> 20
12	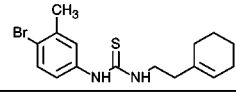	4.6 ± 0.8	9.5 ± 3.0	0.23 ± 0.08
13	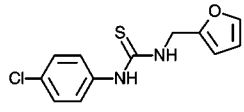	3.4 ± 0.4	5.8 ± 0.8	> 20

Table 1. Continued

Compound[a]		Residual activity (%) [b]		IC_{50} of HIV-1 PV
id	**Structure**	**HIV-1 RT RDDP**	**HIV-1 RT DDDP**	**infection [μM][C]**
14	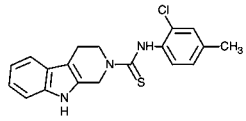	3.7 ± 0.7	9.7 ± 2.4	> 20
15	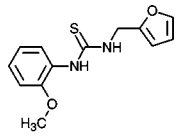	5.9 ± 0.8	11.7 ± 0.5	> 20
16	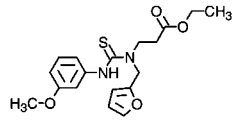	8.5 ± 4.9	35.8 ± 1.1	> 20
17	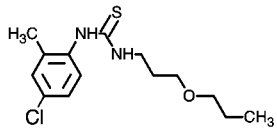	28.0 ± 4.1	52.3 ± 19.9	2.6 ± 0.4

[a] Sixteen molecules were selected on the basis of their inhibition capacity and diversity. Compound **17**, despite exhibiting a residual RDDP activity higher than 15%, was selected from the tested inhibitors, on the basis of its similarity to compound **7** and tested as all other compounds shown. [b] The residual DDDP or RDDP activities were calculated by dividing the residual activity, detected in the presence of a final concentration of specific tested compound of 50 μg/mL, by the initial activity with no inhibitor present and then multiplying the outcome by 100 (expressed as a percentage of initial enzymatic activity with no inhibitor). [c] Concentration inhibiting 50% of HIV-1 pseudovirus (PV) infection.

This time, each compound was tested first for its effect on the DDDP activity of HIV-1 RT as well as for its selectivity of inhibiting this enzyme. This was done by comparing the capacity of each compound to inhibit HIV-1 RT with its effect on the DDDP activity of the Klenow fragment of *Escherichia coli* DNA polymerase I (KF), which served as a distinct and unrelated DNA polymerase. This procedure allowed a side-by-side comparison of the effects of each selected compound on the two enzymes under identical experimental conditions. The specificity of each compound (designated the selectivity index) was calculated by dividing the residual KF activity by that of HIV-1 RT. Compounds with a selectivity index higher than 1 have a higher specificity toward HIV-1 RT, whereas a value lower than 1 indicates a reversed specificity that was directed toward KF. As shown in Table 2, of the total 23 tested compounds, 10 inhibited more than 75% of the DDDP activity of HIV-1 RT (44% of the total molecules) with selectivity index values varying between 0.2 and 7.4. Of these 10 inhibitors, six compounds exhibited a higher specificity toward HIV-1 RT, with a selectivity index of >1, whereas four compounds were more specific toward KF.

Five compounds with a selectivity index of >3 were further tested for their ability to protect human lymphocytes from HIV-1 pseudovirus infection (Table 2). The most potent inhibitor in this group was 1-(4-chloro-2,5-dimethoxyphenyl)-3-(3-propoxypropyl)thiourea (compound **20**). Notably, this molecule included most substituents present also in compounds **7** and **17** (a chlorine and two methoxy substituents), underscoring the significant contribution of each to the inhibition. Efficient inhibition of HIV-1 infection by compound **20** was evident from the reduced fluorescence intensity, which reflected the decline in the level of transduction of the GFP reporter gene, when the compound was incubated with B lymphocytes during HIV-1 pseudovirus infection (see Experimental Section and Figure 1A). The inhibition was dose-dependent and was confirmed by both visualizing the cells under fluorescence microscope and by measuring the fluorescent signal using flow cytometry. In the latter method, the resulting cells could be separated into uninfected and infected cells on the basis of their green fluorescence intensity (Figure 1A). The average fluorescence intensity of the lymphocytes was then plotted against the concentration of compound **20** and fitted into a four-parameter logistic equation with a corresponding IC_{50} value of approximately 168 nM (Figure 1B). As expected, the measured signal was caused by the infecting virions, since cells infected with heat-inactivated pseudovirus did not exhibit any fluorescence above the background level (Figure 1A, bottom panel). The toxicity of compound **20** to B lymphocytes was assayed after incubation for 72 h at 37 °C, under identical experimental conditions used for assaying its inhibitory effect. The concentration of the inhibitor at which cell viability was reduced by 50% compared to the inhibitor-free control (CC_{50} value) was calculated to be ~58 μM, and the resulting CC_{50}/IC_{50} (therapeutic index, TI) value for compound **20** was therefore ~345. Interestingly, the other anti-HIV-1 RT effective compound, **3**, despite being less effective than **20** in inhibiting HIV-1 pseudovirus infection (with an apparent IC_{50} value of ~374 nM), was less toxic than **20** and hence demonstrated a therapeutic index of >446 (Figure 1D). Nevirapine (11-cyclopropyl-5,11-dihydro-4-methyl-6*H*-dipyrido[3,2-*b*:2′,3′*e*][1,4]diazepin-6-one), an NNRTI currently used for HIV-1 therapy, was used as a reference and inhibited HIV-1 in this system with an IC_{50} value of 14 ± 3 nM (data not shown). This inhibition value obtained in our assay was compatible with other values reported for nevirapine, as this drug was shown to inhibit HIV-1 with IC_{50} values of 40 nM for 8186 T-cells,[19] 10−400 nM for MT4 cells,[17,20−22] 24 nM for CEM cells,[23] and 50 nM for 293T cells.[24]

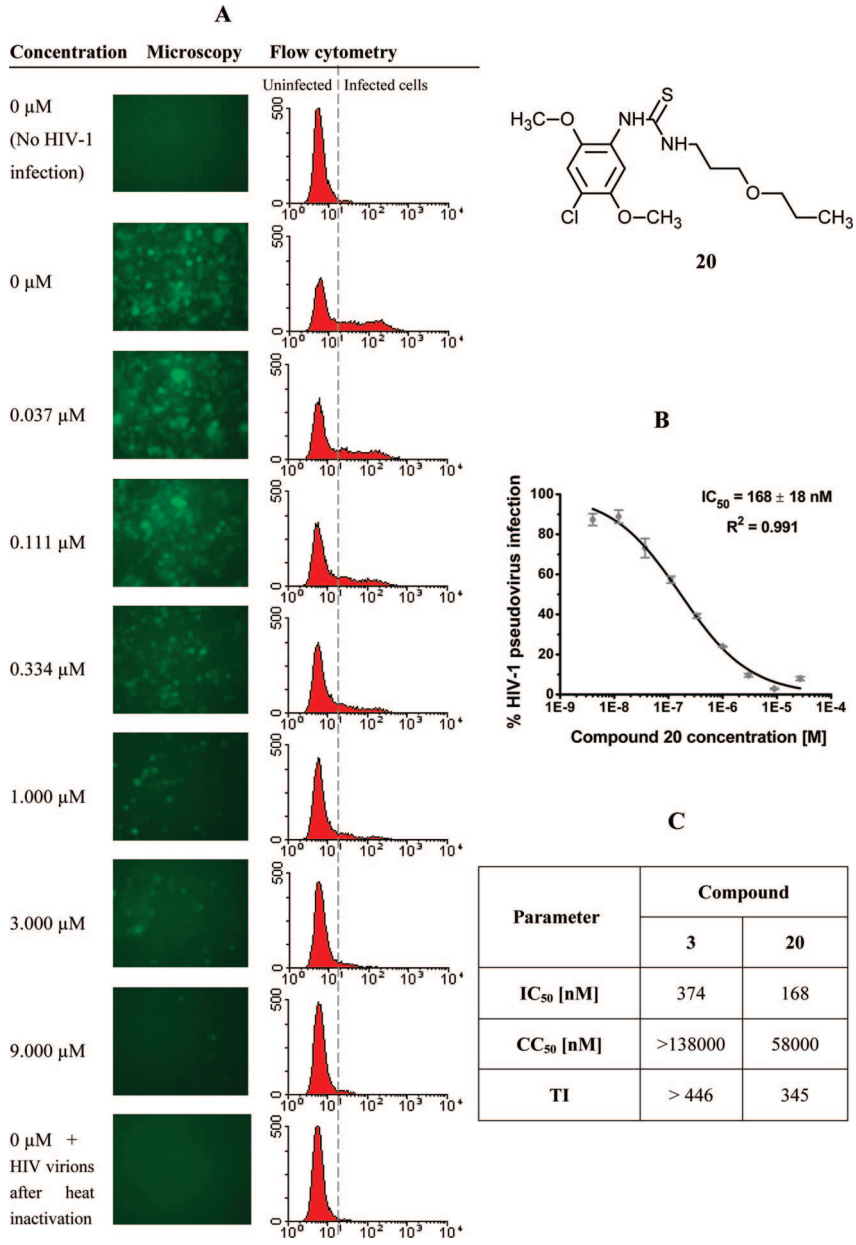

Parameter	Compound	
	3	20
IC_{50} [nM]	374	168
CC_{50} [nM]	>138000	58000
TI	> 446	345

Figure 1. Inhibition activity of compound **20** for the infection of B lymphocytes by HIV-1 pseudovirus. (A) Inhibition effects of different concentrations of compound **20** on HIV-1 infectivity observed through a fluorescence microscope (left column) and measured quantitatively by flow cytometry (right column). (B) Dose−response curve for suppressing viral infectivity and the corresponding IC_{50} value calculated on the basis of the flow cytometry results from panel A. (C) Toxicity and therapeutic index on B lymphocytes of compounds **3** and **20**. CC_{50} is the concentration of inhibitor at which the cell viability was reduced by 50% compared to that of the inhibitor-free control. TI is the therapeutic index (CC_{50}/IC_{50}).

Effect of Compounds 3 and 20 on the Activities of Wild-Type HIV-1 RT, Drug-Resistant Mutants of HIV-1 RT, and Wild-Type HIV-2 RT. As both compounds **3** and **20** efficiently inhibited HIV-1 infection, their RT inhibition capacity was further evaluated. The two compounds were assayed against the three enzymatic activities of recombinant HIV-1 RT: RDDP, DDDP, and RNase H. Compound **3** inhibited the RDDP and DDDP activities with apparent IC_{50} values of ∼2.8 and ∼3.3 μM, respectively (Figure 2). Compound **20** was more potent and inhibited these two DNA polymerase activities with IC_{50} values of approximately 0.51 and 0.94 μM, respectively. The reference NNRTI drug, nevirapine, exhibited IC_{50} values of ∼1.7 and ∼0.63 μM for the RDDP and DDDP activities, respectively. As one would expect, neither compound (including nevirapine) significantly inhibited the RNase H activity of RT, similar to most NNRTIs. Interestingly, the Y181C mutant of HIV-1 RT, which is highly resistant to nevirapine, was also inhibited by the two novel NNRTIs described in this study, albeit less efficiently than wild-type RT (Figure 3). Both new inhibitors were more effective than nevirapine in inhibiting this drug-resistant HIV-1 RT mutant, as the apparent IC_{50} values for compounds **3** and **20** were approximately 20 and 70 μM, respectively, while nevirapine inhibited this mutant with an IC_{50} of ∼100 μM. Further analyses have revealed that the two new anti-HIV-1 compounds were less effective and exhibited an inhibition efficiency similar to that of nevirapine against the double mutant L100I/K103N HIV-1 RT, which is another common NNRTI-resistant variant (data not shown). These results support the conclusion that compounds **3** and **20** interact, at least in part, with the HIV-1 RT binding pocket that is common to most NNRTIs. In addition, both com-

Table 2. Structure−Activity Relationship of 1-(3-Propoxypropyl)thiourea Derivatives

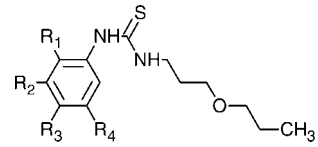

					residual DDDP activity (%)[a]			
	R_1	R_2	R_3	R_4	HIV-1 RT	KF	selectivity index[b]	IC_{50} of HIV-1 PV infection (μM)[c]
18	F	H	H	F	82.3 ± 12.3	47.5 ± 13.4	0.6 ± 0.2	
19	H	H	Br	CH_3	24.8 ± 6.3	14.4 ± 3.4	0.6 ± 0.2	
20	OCH_3	H	Cl	OCH_3	8.4 ± 2.2	62.2 ± 14.4	7.4 ± 2.6	0.17 ± 0.02
21	H	H	Br	H	27.8 ± 3.2	48.4 ± 18.5	1.7 ± 0.7	
22	Cl	H	H	CH_3	17.3 ± 0.8	76.5 ± 13.8	4.4 ± 0.8	0.67 ± 0.08
23	H	H	$(CH_2)_3CH_3$	H	31.4 ± 13.7	74.2 ± 3.2	2.4 ± 1.0	
24	H	H	Cl	CF_3	4.4 ± 2.8	2.2 ± 1.7	0.5 ± 0.5	
25	CH_3	Cl	H	H	28.9 ± 12.9	10.8 ± 5.2	0.4 ± 0.2	
26	CH_3	H	$(CH_2)_3CH_3$	H	27.5 ± 7.7	4.5 ± 1.2	0.2 ± 0.1	
27	OCH_2CH_3	H	H	H	16.2 ± 0.2	87.1 ± 10.1	5.4 ± 0.6	0.43 ± 0.07
28	OCH_3	H	H	CH_3	16.7 ± 0.2	71.7 ± 6.4	4.3 ± 0.4	0.89 ± 0.11
29	H	H	$COOCH_3$	H	13.6 ± 3.8	2.6 ± 1.7	0.2 ± 0.1	
30	Br	H	F	H	39.4 ± 10.3	47.6 ± 11.0	1.2 ± 0.4	
31	H	H	$C(CH_3)_3$	H	34.3 ± 19.9	13.8 ± 1.8	0.4 ± 0.2	
32	H	H	H	OCH_3	30.5 ± 3.5	98.7 ± 9.4	3.2 ± 0.5	
33	H	H	H	CN	69.0 ± 1.5	75.2 ± 27.3	1.1 ± 0.4	
34	Cl	H	H	H	49.2 ± 4.8	59.3 ± 19.3	1.2 ± 0.4	
35	CH_3	H	CH_3	CH_3	21.9 ± 0.7	64.4 ± 3.3	2.9 ± 0.2	
36	H	H	H	$COO\ CH_2CH_3$	47.1 ± 11.8	56.6 ± 14.4	1.2 ± 0.4	
37	Cl	H	Cl	H	53.4 ± 7.8	13.2 ± 6.4	0.2 ± 0.1	
38	H	H	Br	Cl	5.5 ± 0.4	1.0 ± 0.7	0.2 ± 0.1	
39	OCH_3	H	H	Cl	15.7 ± 0.8	50.8 ± 12.3	3.2 ± 0.8	0.32 ± 0.11
40	H	H	$N(CH_3)_2$	H	55.0 ± 7.0	11.1 ± 1.4	0.2 ± 0.0	

[a] Same as footnote b in Table 1. [b] The selectivity index is the percent residual KF-derived DDDP activity divided by the percent residual HIV-1 RT-derived DDDP activity. [c] Same as footnote c in Table 1. Calculated only for the selected compounds for which the values are shown.

pounds also inhibited ∼50% of HIV-2 RT activity at 140 μM, a feature that is not shared by most classic NNRTIs, such as nevirapine[25] (Figure 3).

Reversibility of HIV-1 RT Inhibition by Compound 20. The mode by which compound **20**, which was the most efficient inhibitor of wild-type HIV-1 RT, inhibited RT was further evaluated. To test the reversibility of the binding between HIV-1 RT and compound **20**, we assayed the RDDP activity of RT at increasing concentrations of the enzyme in the absence or presence of 616 nM inhibitor (Figure 4). Plotting HIV-1 RT concentrations against their apparent V_{max} values for the reactions with and without the inhibitor showed intersecting rather than parallel lines. In other words, the RT activity in the presence of compound **20** was proportionally increased as a function of RT concentration with 59 ± 6% residual activity at all tested RT concentrations. This excluded the possibility that a fraction of RT was irreversibly eliminated by the inhibitor and suggested a reversible binding between RT and compound **20**.

Mode of Inhibition of the RDDP Activity of HIV-1 RT by Compound 20. To gain better insight into the mechanism by which HIV-1 RT is inhibited by compound **20**, steady state kinetic studies were performed by assaying the RDDP activity of wild-type HIV-1 RT in the presence of increasing concentrations of each substrate that was used (either dTTP or rA·dT) and a specific concentration of the inhibitor. These assays were repeated with a range of compound **20** concentrations, and the results were analyzed with double-reciprocal (Lineweaver−Burk) plots. RT inhibition with respect to both substrates showed a classical noncompetitive behavior with no significant change in the apparent K_m values in the presence of compound **20** (Figure 5). In the kinetic study with respect to the dTTP substrate (Figure 5A,B), the control calculated value for the reaction without inhibitor was 4.3 μM dTTP, whereas the calculated K_m values in the presence of 0.25, 0.5, 1, and 2 μM compound **20** were 4.5, 4.8, 4.3, and 4.2 μM, respectively (average of 4.5 ± 0.25 μM). In accordance with this mode of inhibition, the k_{cat} values (V_{max}/[RT]) were decreased by the compound from approximately 0.38 s^{-1} in the absence of inhibitor to 0.28, 0.25, 0.20, and 0.13 s^{-1} in the presence of 0.25, 0.5, 1, and 2 μM compound **20**, respectively. In the second kinetic study with respect to the rA·dT substrate (Figure 5C,D), a similar pattern was observed with a K_m value of 0.100 μg/mL for the control reaction and K_m values of 0.096 ± 0.001 μg/mL for 0.25, 0.5, 1, and 2 μM compound **20**. In this case, the k_{cat} values could not be calculated in the standard units of inverse seconds, due to the heterogeneous length of the commercial substrate [poly(rA)$_n$·oligo(dT)$_{12-18}$]. Further analysis of both kinetic studies via a repotting the $1/V_{max}$ values against the inhibitor concentrations (Dixon plot) showed a linear trend with a high correlation coefficient (r^2) of 0.99. The K_i values calculated from these plots yielded a value of 1.1 μM with respect to the dTTP substrate and 1.8 μM with respect to the rA·dT substrate (Figure 5B,D). On the basis of these data, it is likely that neither the dTTP substrate nor the rA·dT substrate competed with the inhibitor for binding to the enzyme and each of the molecules could bind RT independently.

Discussion

In this study, we have demonstrated that in silico virtual screening against two different crystal structures of HIV-1 RT can underscore compounds with a high probability of inhibiting the infection of sensitive cells by HIV-1. Virtual screening by itself may not always guarantee a successful identification of potent inhibitors against HIV-1 RT and may therefore require additional complementary approaches.[26] To permit a more

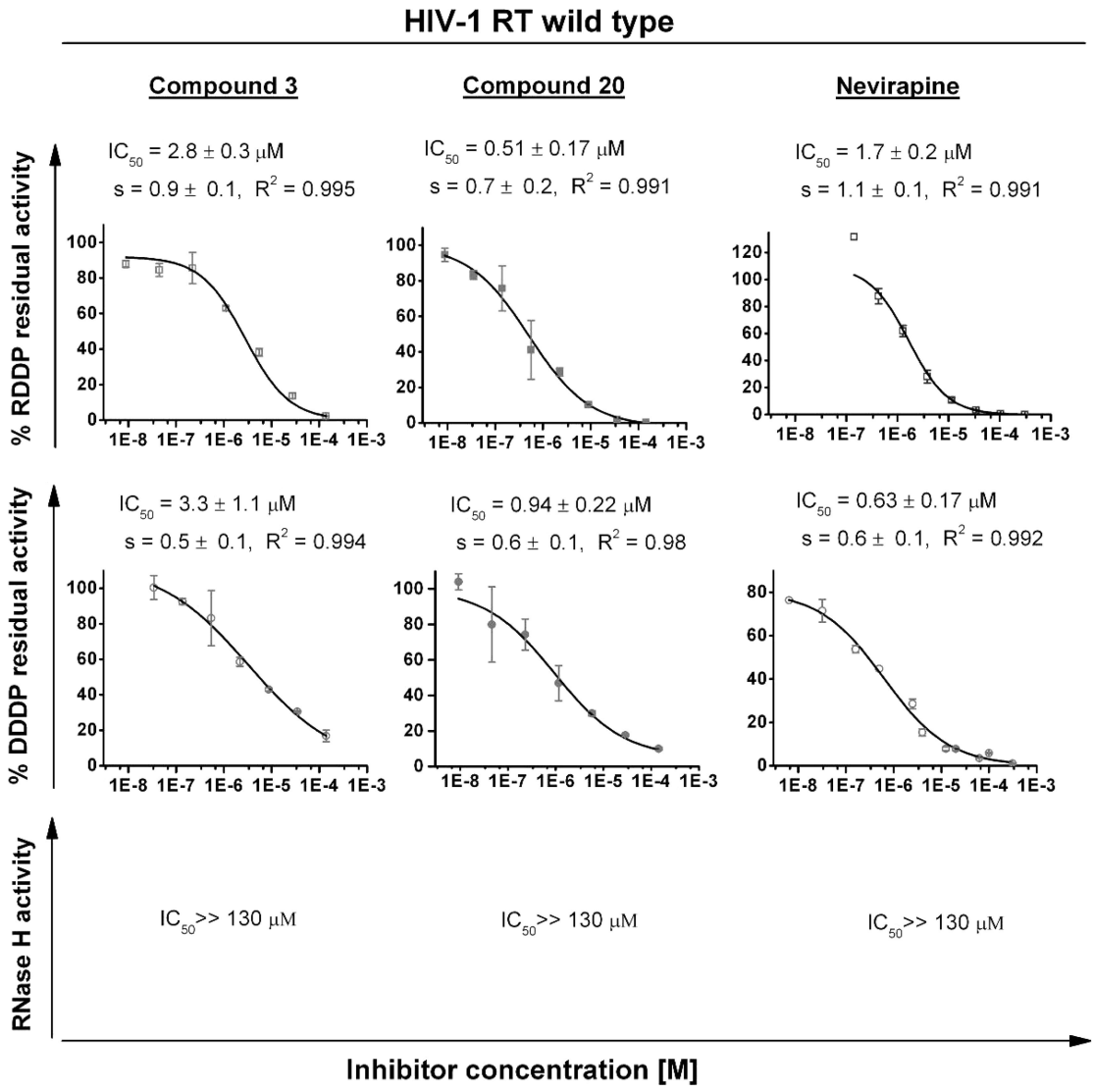

Figure 2. Effects of compounds **3**, **20** and nevirapine on the enzymatic activities of wild-type HIV-1 RT. The RDDP, DDDP, and RNase H activities of wild-type HIV-1 RT were assayed in the presence of increasing concentrations of the specified inhibitors (from top to bottom). The dose−response curves for each inhibitor were fitted to a four-parameter logistic equation, and the IC_{50} parameters as well as standard errors, sigmoidity, and correlation coefficients are reported. The reference results for the inhibition of the RDDP activity of wild-type HIV-1 RT, as well as the DDDP activity, by nevirapine were taken from our previous studies. Reproduced from refs 15 and 16. Copyright 2007 and 2008, respectively, American Chemical Society.

stringent screen that can lead to more reliable results, we used two different structures of HIV-1 RT for docking, as we have previously described.[16] Interestingly, some compounds found in this study, designated **1**, **5**, **9**, **12**, **13**, and **15**, share similar structural elements with the known NNRTI, PETT. PETT-1, which is a derivative of PETT, was actually the original inhibitor in the HIV-1 RT structure, 1dtq,[18] that was used in this study. Thus, the docking process used by us could retrieve compounds that resembled the original inhibitor, confirming the reliability and reproducibility of this docking procedure. In the study presented here, this approach has successfully led to identification of several novel compounds that inhibit HIV-1 infection at nanomolar concentrations (Tables 1 and 2).

Moreover, a structure−activity relationship study resulted in several improved compounds and enabled us to link a specific atom identity and spatial position to the inhibition efficacy. For example, both compounds **17** and **22** carry the identical atoms but differ in the orientation of their substituents. In compound **22**, the methyl group is shifted from the ortho to the meta position and the chloride atom is shifted from the para to the ortho position (both on the single aromatic ring of the compound) relative to compound **17**. Evidently, these modifications were beneficial as compound **22** inhibited HIV-1 pseudovirus infection with an IC_{50} value of ~0.67 μM, which was ~4-fold lower than the IC_{50} value of compound **17** (2.6 μM). This effect cannot be attributed to only the shift in the chloride atom position, as compound **34**, which carries only the chloride at the ortho position [in addition to the 1-(3-propoxypropyl)thiourea group], exhibited only moderate inhibition of HIV-1 RT that resulted in only ~50% residual activity. Five 1-(3-propoxypropyl)thiourea derivatives, which inhibited both HIV-1 RT and HIV-1 PV infection, were found in the original Leadquest3 library. They were not selected in the initial virtual screening but were identified later on the basis of their similarity to screened compounds that inhibited HIV. Two of them (**22** and **39**) scored high values in the docking process, yet not high enough to be selected by the virtual screening. The docking of the other three compounds (**20**, **27**, and **28**) resulted in crash values below the threshold used (less than −3; see Experimental Section), and consequently, they were also excluded from the

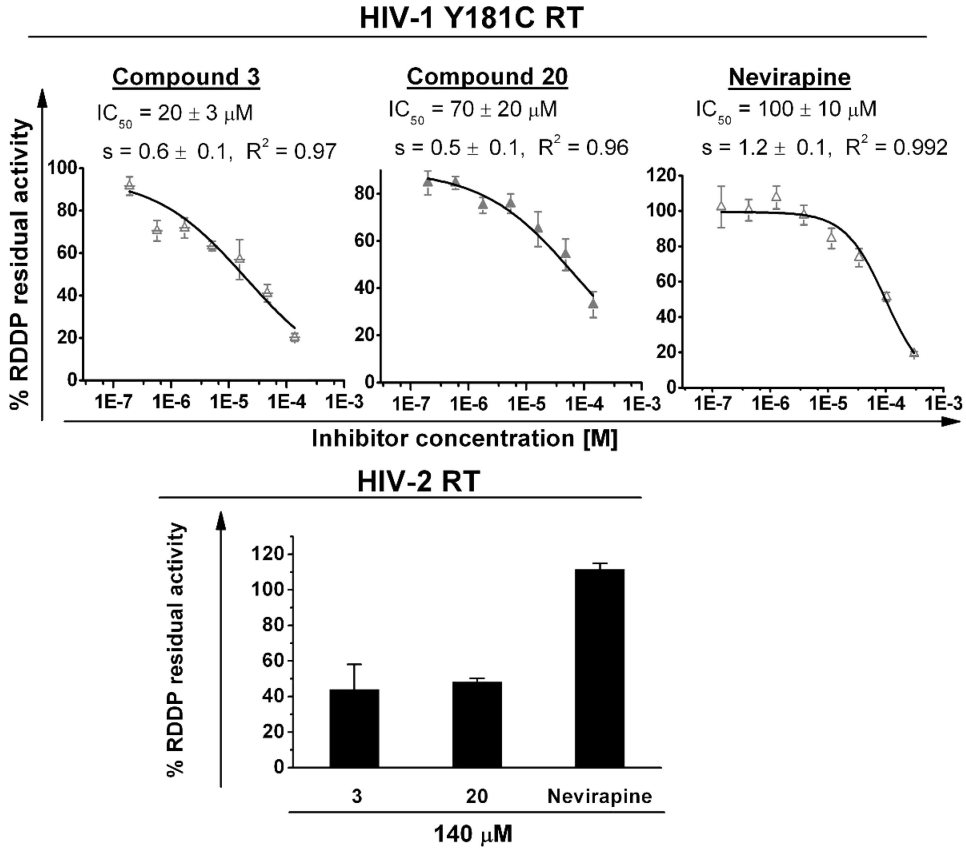

Figure 3. Effects of compounds **3**, **20** and nevirapine on the enzymatic activities of the Y181C mutant of HIV-1 RT and wild-type HIV-2 RT. The RDDP activity of Y181C HIV-1 RT and wild-type HIV-2 RT was tested in the presence of the different inhibitors. The dose−response curves for each inhibitor were fitted to a four-parameter logistic equation, and the IC_{50} parameters as well as standard errors, sigmoidicity, and correlation coefficients are reported. The reference results for the inhibition of the RDDP activity of Y181C HIV-1 RT by nevirapine were taken from ref 15. Copyright 2007 American Chemical Society.

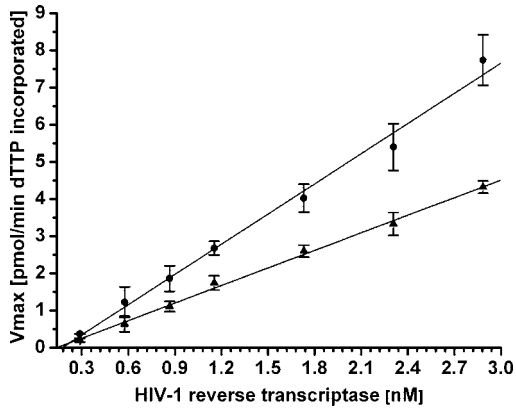

Figure 4. Maximal velocity of HIV-1 RT-associated DNA polymerase activity as a function of enzyme concentration. The DNA polymerase activity was monitored by assessing the poly(rA)$_n$•oligo(dT)$_{12-18}$-dependent incorporation of [^{3}H]dTTP into nascent DNA in the absence (●) or presence (▲) of 616 nM compound **20**. RT activity was assayed for 15 min at 37 °C, and the extent of [^{3}H]dTTP incorporation was determined as described in Experimental Section. The curves were fitted by linear regression analysis that resulted in high correlation coefficients (r^2) of 0.995 without inhibitor and 0.998 with the inhibitor, indicating a strong linear relationship between V_{max} values and enzyme concentrations.

selection. Apparently, these crashes could be well-accommodated in the hydrophobic pocket of the RT in solution, as the compounds efficiently inhibited HIV-1 RT activity. In this case, a rational analysis of the inhibition capacity of the initially selected compounds was further required to identify this group of inhibitors. The two most efficient compounds were intensively characterized and exhibited a diminished efficacy in inhibiting HIV-1 RT variants with mutations in residues that participate in the formation of the NNRTI hydrophobic binding pocket of the RT. On the basis of this information, we conclude that these inhibitors probably interact primarily with this NNRTI-binding site (despite inhibiting an NNRTI-resistant RT mutant better than nevirapine).

To define the molecular interactions of compounds **3** and **20** with HIV-1 RT, we have further inspected the conformation for docking of these molecules into a crystal structure of HIV-1 RT (PDB entry 1dtq). Both compounds could fit quite well into the NNRTI hydrophobic pocket (Figure 6), interacting with several RT residues. Compound **20** formed two hydrogen bonds with HIV-1 RT, where the hydrogen atoms attached to the two thiourea nitrogens interacted with the carbonyl oxygen of two different RT residues. One bond formed with the Glu138 side chain, located in the p51 subunit of HIV-1 RT, while the other one formed with the carbonyl backbone of Lys101, located in the p66 subunit. Notably, the interaction with Lys101 of HIV-1 RT was experimentally observed for several NNRTIs[5] and further supports the accuracy of the model presented herein. Compound **3** also formed two hydrogen bonds, one with Glu138 of the p51 RT subunit and another with the hydroxyl group of Tyr318 in the larger (p66) subunit. Tyr318 is highly conserved in HIV-1 RT and makes contact within 4 Å with most NNRTIs that bind the hydrophobic pocket.[27] The importance of a tyrosine at this position was evident from a mutagenesis analysis, where only the RT mutant, in which this residue was replaced with

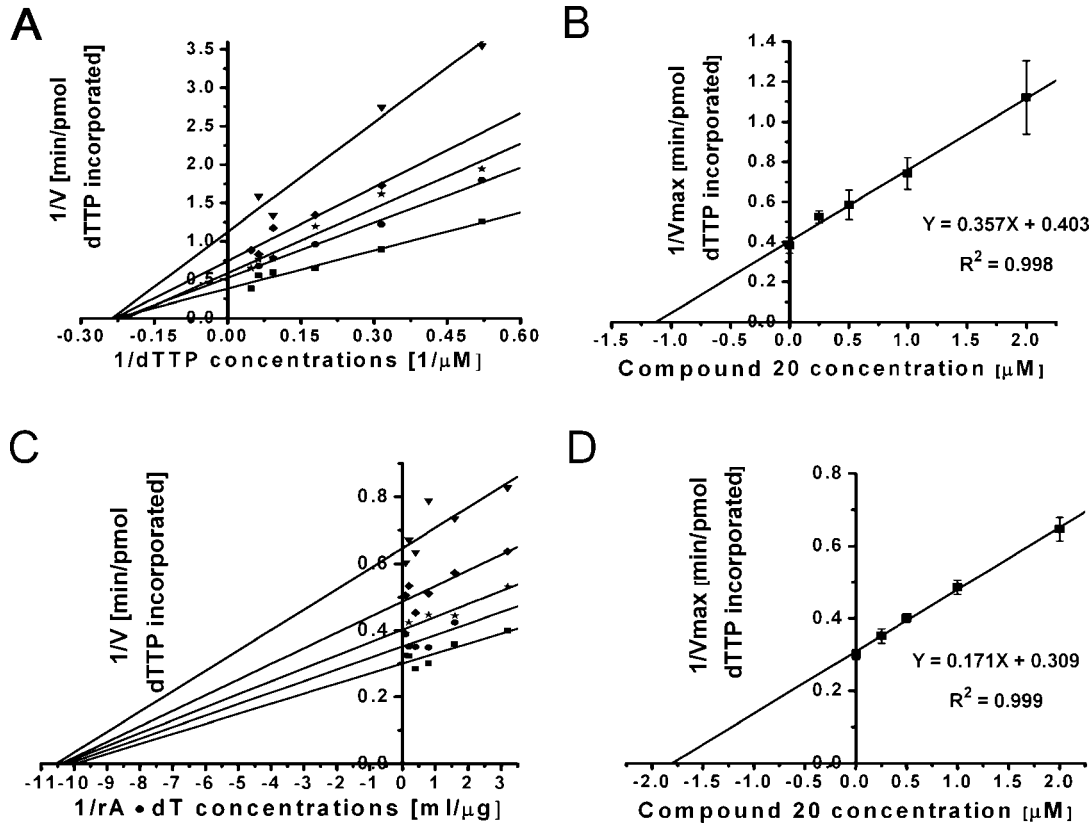

Figure 5. Kinetic analysis of the inhibition of HIV-1 RT-associated DNA polymerase activity by compound **20** with respect to either the dTTP substrate or the rA•dT template. (A) Double-reciprocal plot of the initial velocity of the RDDP activity of HIV-1 RT as a function of dTTP substrate concentration. Increasing concentrations of dTTP in the absence (■) or presence of 0.25 (●), 0.5 (★), 1 (◆), or 2 μM compound **20** (▼). (B) Replot (Dixon plot) of the reciprocal maximal velocity (calculated from panel A) vs various concentrations of compound **20**. The kinetic constants K_m and K_i were calculated by using linear regression analysis. Panels C and D are similar to panels A and B, respectively, but with the rA•dT template.

either Phe or Trp (of six total residues tested at position 318 of p66) retained any substantial RT activity.[27] While the Y318F RT mutant still retained a substantial sensitivity to the majority of the NNRTIs tested, the Y318W mutant showed varying degrees of resistance to different NNRTIs.[27] The E138K mutation in HIV-1 RT was also reported to lead to resistance to derivatives of [2′,5′-bis-*O*-(*tert*-butyldimethylsilyl)-3′-spiro-5″-(4″-amino-1″,2″-oxathiole-2″,2″-dioxide)]-β-D-pentofuranosyl (TSAO), while retaining sensitivity to other NNRTIs, such as nevirapine.[28]

The two compounds, which efficiently inhibited recombinant HIV-1 RT and viral infection, although sharing a few functional groups with previously identified NNRTIs,[9,18] are novel HIV-1 RT inhibitors. Compound **3** contains a unique benzothiadiazole ring, whereas compound **20** contains a unique long chain and several substituents on the ring not found in any of the PETT derivatives. We are currently designing various analogues of compounds **3** and **20** that will be tested against wild-type HIV-1 RT and known NNRTI drug-resistant mutants. We are hopeful that this could result in new leads for the development of novel drugs for treatment of HIV-1 carriers and AIDS patients.

Experimental Section

Virtual Screening. The Tripos library of "druglike" compounds was docked into HIV-1 RT structures in two steps as previously described.[16] First, three components were prepared for the docking process: RT structures, an idealized binding site in each RT (a protomol), and an optimized conformation of each compound in the library. RT structures [PDB entries 1fk9[29] and 1dtq[18]] were downloaded from the Research Collaboratory for Structural Bioinformatics site, and their bound inhibitors were removed, followed by addition of any missing hydrogen atoms. Due to the long computational procedure required to screen each RT structure against all compounds in the large library, only two structures were used. Protomol was generated using the location of the original inhibitor and the defaults setting of Surflex. The Tripos Leadquest3 library was downloaded as a structure data (sd) file. Each compound was then energy-minimized with Omega (Openeye software) into a single optimized conformation, using the mmff94s force field.[30] All compounds were saved in their optimized conformation in a mol2 file that retains their spatial coordinates in space. The three files containing HIV-1 RT structures, protomol, and the conformation of each compound were used as an input to the docking process. Docking was performed by fragmenting each molecule and fitting the conformation of each fragment into the protomol to yield a spatial structure that maximizes molecular similarity to the protomol.[31] The 10 top conformations for each compound were retrieved according to their score as output files. These included a log output file with the scores for each conformation and a structural output file with the coordinates for the suggested conformations. All retrieved compounds were then filtered from the log output file using thresholds of 6 for score values, −3 for crash values, and 1 for polar values, with Filter. Docking conformations of filtered top compounds were extracted from the structural output file with Extract. Filter and Extract were written in Perl to filter and extract, respectively, specific conformations of specific compounds from the results file; both are available upon request. This process was repeated with both RT structures, and the molecules were then ranked on the basis of their average scores over the two structures. In addition to selecting compounds according to the procedure described above, several other compounds with exceptionally high scores against only one RT structure, and additional compounds

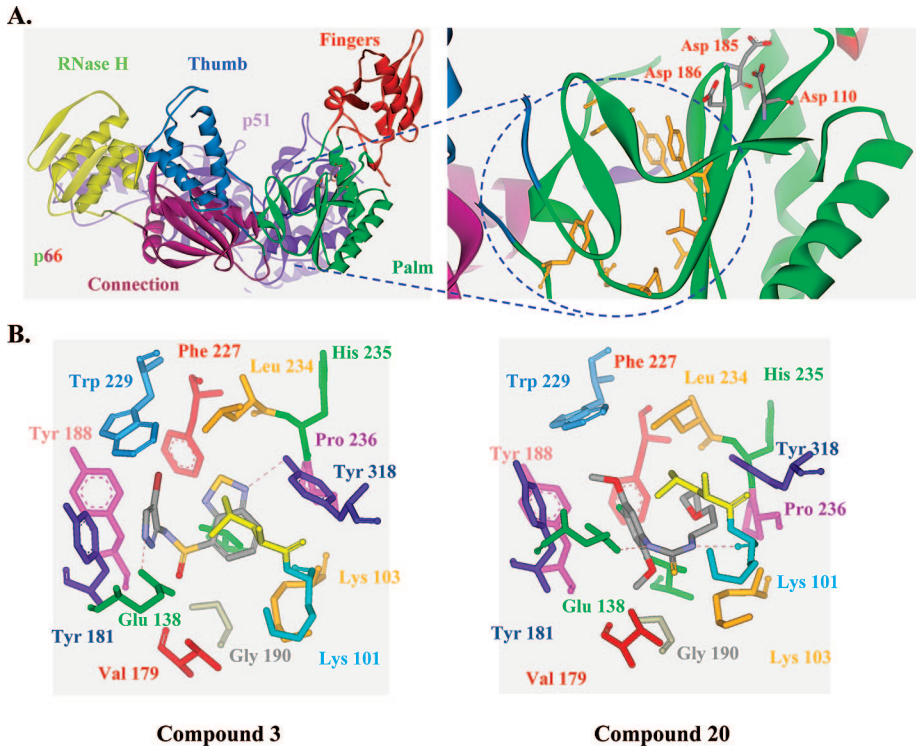

Figure 6. Docking of compounds **3** and **20** into the NNRTI binding site of wild-type HIV-1 RT. (A) Spatial structure of wild-type HIV-1 RT with its defined subdomains (left, each subdomain in the p66 subunit is depicted in a different color while the p51 is positioned behind the p66) and the location of the hydrophobic pocket along with the three aspartic acids that form the catalytic site of the DNA polymerase domain (right). (B) Compounds **3** (left) and **20** (right) were docked into the HIV-1 RT structure as found in PDB entry 1dtq using Surflex. The top-scoring conformation of each molecule is shown. Amino acids in the pocket are specified in three-letter codes and different colors; Glu138 is part of the p51 HIV-1 RT subunit, and all the other amino acids are part of the p66 subunit. The two compounds are depicted in CPK (Corey, Pauling, and Kultin) colors and are displayed as a stick model. All structures were displayed with discovery studio visualizer 1.6(Accelrys Software Inc.).

with a high ratio of docking score to the number of rotational bonds, were all added to the list. Each docking was further analyzed visually with discovery studio visualizer 1.6 (Accelrys Software Inc.). All compounds selected for further biochemical analyses were purchased from Tripos Inc.

Expression and Purification of RTs. Recombinant wild-type p66/p51 HIV-1 RT, derived from the BH10 clone, was expressed in bacteria as previously described.[32] The expression plasmids, encoding the single RT mutant Y181C and the double mutant L100I/K103N, were a generous gift from S. Hughes of the National Cancer Institute (National Institutes of Health, Frederick, MD). The Y181C mutant of HIV-1 RT was expressed in *E. coli* BL-21, and the L100I/K103N double mutant was expressed in *E. coli* DH5α. Both RT mutants were purified in a manner similar to the purification of wild-type HIV-1 RT. Heterodimeric (p68/p55) HIV-2 RT was expressed and purified by us as described.[32,34] The Klenow fragment of *E. coli* DNA polymerase I (KF) was purchased from New England Biolabs.

Quantitative Assays for RT and KF Activities. The RDDP activity of RT was assayed by assessing the incorporation of [^{3}H]dTTP into the poly(rA)$_n$·oligo(dT)$_{12-18}$ template·primer, as previously described.[33] All reactions were performed at 37 °C in a final volume of 100 μL that included 1% DMSO. To avoid exposure of RT to high local DMSO concentrations, 1 μL of each inhibitor, dissolved in concentrated DMSO (or 1 μL of DMSO as a control), was added to 79 μL of the reaction buffer and mixed, and only then were the rest of the other reaction components, including RT, added. The DDDP activity of either RT or KF was assayed in a similar manner but with activated herring sperm DNA at the final concentration of 20 μg/mL, substituting the synthetic template·primer and with all four dNTPs present in the reaction mixture.[34] The DDDP activity of RT and of KF was assayed under identical experimental conditions. Reported values in this research are all averages of the results of three independent experiments.

The HIV-1 RT-associated RNase H activity was assayed by fluorescence resonance energy transfer technology as described previously.[35] Briefly, HIV-1 RT was incubated with a substrate hybrid of fluorescein-RNA and DNA-4-{[4′-(dimethylamino)phenyl]azo}benzoic acid and with (or without) a specific inhibitor. Hydrolysis of the substrate and the resulting emitting fluorescence were measured with a fluorescence spectrometer after incubation for 30 min at 37 °C. To improve the signal-to-noise ratio, the assay was slightly modified to contain 6 nM RT and 1 mM DTT. All measurements were conducted in triplicate in a 96-well plate.

Steady State Kinetic RDDP Assays. All kinetic assays were conducted as described above for the quantitative analysis, with different concentrations of either dTTP or poly(rA)$_n$·oligo(dT)$_{12-18}$ template·primer as indicated.[36,37] Reaction mixtures were incubated for 15 min, and the results were linearly fitted using Origin 7.5.

Cytotoxicity Assay. This assay was performed as previously described.[38] Target B lymphocytes (721.221 cells) were incubated in a 96-well plate with various inhibitor concentrations (each concentration in triplicate) at 37 °C for 72 h. Cell viability was then assayed using the XTT substrate. Absorbance was recorded at 450 nm, and the reference wavelength was recorded at 620 nm.

HIV-1 Pseudovirus Infection. Infectious virions were prepared by transfecting 293T cells with three plasmids: pCMVΔ-R8.2Gagpol,[39] which encodes HIV-1 proteins (except for Env); pHRCMVGFP, which is transcribed to mRNA containing encapsidation signal and the GFP coding sequences; and pVSV-G, which supplies an envelope protein that is able to infect a wide variety of cells. Chloroquine, to a final concentration of 25 μM, was added to the medium prior to transfection, and 48 h post-transfection, the supernatant was collected, filtered through a 0.45 μm filter, equilibrated with 50 mM HEPES (pH 7.2), and stored at −80 °C. Virions were unfrozen at 37 °C and allowed to infect B lymphocytes (721.221 cells) in the presence of 5.6 μg/mL Polybrene and a

specific inhibitor concentration at a final concentration of 1% DMSO in RPMI medium. Between 48 and 72 h post-infection, the cells were collected, fixed with 1% paraformaldehyde, and analyzed by flow cytometry (BD Biosciences) or fluorescence microscopy. The values reported are from four independent experiments for compounds **20** and **3** and three experiments for all other compounds.

Acknowledgment. This research was supported in part by a grant from the Saia Foundation on HIV research at Tel Aviv University. We thank Dr. E. Bacharach from Tel Aviv University for supplying the HIV-1 pseudovirus system, Dr. S. H. Hughes from the National Cancer Institute for sending the plasmids that express the mutant HIV-1 RTs studied here, Dr. A. N. Jain from the University of California (San Francisco, CA) for supplying Suflex, Open Eye Inc. for Omega, Dr. O. Mandelboim from the Hebrew University for the 721.221 cells, and Dr. M. Parniak from the University of Pittsburgh (Pittsburgh, PA) for the RNase H assay system. We are also grateful to the AIDS Research and Reference Reagent Program, Division of AIDS, NIAID, NIH, for nevirapine. Specials thanks to Prof. A. Nudelman of Bar Ilan University and to Dr. I. Oz-Gleenberg from our laboratory for critical reading of the manuscript. A. Herschhorn was supported by the Tel Aviv University President and Rector Scholarship for excellence. A. Hizi is the Incumbent of the Gregorio and Dora Shapira Chair for the Research of Malignancies.

Supporting Information Available: Tripos code numbers of all compounds used in this study. This material is available free of charge via the Internet at http://pubs.acs.org.

References

(1) De Clercq, E. Antiviral drugs in current clinical use. *J. Clin. Virol.* **2004**, *30*, 115–133.
(2) De Clercq, E. HIV-chemotherapy and -prophylaxis: New drugs, leads and approaches. *Int. J. Biochem. Cell Biol.* **2004**, *36*, 1800–1822.
(3) De Clercq, E. Antivirals and antiviral strategies. *Nat. Rev. Microbiol.* **2004**, *2*, 704–720.
(4) Coffin, J. M.; Hughes, S. H.; Varmus, H. E. *Retroviruses*, Cold Spring Harbor Laboratory Press, Plainview, NY, 1997.
(5) Das, K.; Lewi, P. J.; Hughes, S. H.; Arnold, E. Crystallography and the design of anti-AIDS drugs: Conformational flexibility and positional adaptability are important in the design of non-nucleoside HIV-1 reverse transcriptase inhibitors. *Prog. Biophys. Mol. Biol.* **2005**, *88*, 209–231.
(6) Sarafianos, S. G.; Das, K.; Hughes, S. H.; Arnold, E. Taking aim at a moving target: Designing drugs to inhibit drug-resistant HIV-1 reverse transcriptases. *Curr. Opin. Struct. Biol.* **2004**, *14*, 716–730.
(7) Das, K.; Clark, A. D., Jr.; Lewi, P. J.; Heeres, J.; De Jonge, M. R.; Koymans, L. M.; Vinkers, H. M.; Daeyaert, F.; Ludovici, D. W.; Kukla, M. J.; De Corte, B.; Kavash, R. W.; Ho, C. Y.; Ye, H.; Lichtenstein, M. A.; Andries, K.; Pauwels, R.; De Bethune, M. P.; Boyer, P. L.; Clark, P.; Hughes, S. H.; Janssen, P. A.; Arnold, E. Roles of conformational and positional adaptability in structure-based design of TMC125-R165335 (etravirine) and related non-nucleoside reverse transcriptase inhibitors that are highly potent and effective against wild-type and drug-resistant HIV-1 variants. *J. Med. Chem.* **2004**, *47*, 2550–2560.
(8) Janssen, P. A.; Lewi, P. J.; Arnold, E.; Daeyaert, F.; de Jonge, M.; Heeres, J.; Koymans, L.; Vinkers, M.; Guillemont, J.; Pasquier, E.; Kukla, M.; Ludovici, D.; Andries, K.; de Bethune, M. P.; Pauwels, R.; Das, K.; Clark, A. D., Jr.; Frenkel, Y. V.; Hughes, S. H.; Medaer, B.; De Knaep, F.; Bohets, H.; De Clerck, F.; Lampo, A.; Williams, P.; Stoffels, P. In search of a novel anti-HIV drug: Multidisciplinary coordination in the discovery of 4-[[4-[[4-[(1E)-2-cyanoethenyl]-2,6-dimethylphenyl]amino]-2- pyrimidinyl]amino]benzonitrile (R278474, rilpivirine). *J. Med. Chem.* **2005**, *48*, 1901–1909.
(9) Masuda, N.; Yamamoto, O.; Fujii, M.; Ohgami, T.; Fujiyasu, J.; Kontani, T.; Moritomo, A.; Orita, M.; Kurihara, H.; Koga, H.; Kageyama, S.; Ohta, M.; Inoue, H.; Hatta, T.; Shintani, M.; Suzuki, H.; Sudo, K.; Shimizu, Y.; Kodama, E.; Matsuoka, M.; Fujiwara, M.; Yokota, T.; Shigeta, S.; Baba, M. Studies of non-nucleoside HIV-1 reverse transcriptase inhibitors. Part 2: Synthesis and structure-activity relationships of 2-cyano and 2-hydroxy thiazolidenebenzenesulfonamide derivatives. *Bioorg. Med. Chem.* **2005**, *13*, 949–961.
(10) Romines, K. R.; Freeman, G. A.; Schaller, L. T.; Cowan, J. R.; Gonzales, S. S.; Tidwell, J. H.; Andrews, C. W., III; Stammers, D. K.; Hazen, R. J.; Ferris, R. G.; Short, S. A.; Chan, J. H.; Boone, L. R. Structure-activity relationship studies of novel benzophenones leading to the discovery of a potent, next generation HIV nonnucleoside reverse transcriptase inhibitor. *J. Med. Chem.* **2006**, *49*, 727–739.
(11) Cao, J.; Isaacson, J.; Patick, A. K.; Blair, W. S. High-throughput human immunodeficiency virus type 1 (HIV-1) full replication assay that includes HIV-1 Vif as an antiviral target. *Antimicrob. Agents Chemother.* **2005**, *49*, 3833–3841.
(12) Jochmans, D.; Deval, J.; Kesteleyn, B.; Van Marck, H.; Bettens, E.; De Baere, I.; Dehertogh, P.; Ivens, T.; Van Ginderen, M.; Van Schoubroeck, B.; Ehteshami, M.; Wigerinck, P.; Gotte, M.; Hertogs, K. Indolopyridones inhibit human immunodeficiency virus reverse transcriptase with a novel mechanism of action. *J. Virol.* **2006**, *80*, 12283–12292.
(13) Romero, D. L.; Busso, M.; Tan, C. K.; Reusser, F.; Palmer, J. R.; Poppe, S. M.; Aristoff, P. A.; Downey, K. M.; So, A. G.; Resnick, L.; Tarpley, W. Nonnucleoside reverse transcriptase inhibitors that potently and specifically block human immunodeficiency virus type 1 replication. *Proc. Natl. Acad. Sci. U.S.A.* **1991**, *88*, 8806–8810.
(14) Wyatt, P. G.; Bethell, R. C.; Cammack, N.; Charon, D.; Dodic, N.; Dumaitre, B.; Evans, D. N.; Green, D. V.; Hopewell, P. L.; Humber, D. C.; Lamont, R. B.; Orr, D. C.; Plested, S. J.; Ryan, D. M.; Sollis, S. L.; Storer, R.; Weingarten, G. G. Benzophenone derivatives: A novel series of potent and selective inhibitors of human immunodeficiency virus type 1 reverse transcriptase. *J. Med. Chem.* **1995**, *38*, 1657–1665.
(15) Herschhorn, A.; Lerman, L.; Weitman, M.; Gleenberg, I. O.; Nudelman, A.; Hizi, A. De novo parallel design, synthesis and evaluation of inhibitors against the reverse transcriptase of human immunodeficiency virus type-1 and drug-resistant variants. *J. Med. Chem.* **2007**, *50*, 2370–2384.
(16) Herschhorn, A.; Oz-Gleenberg, I.; Hizi, A. Mechanism of inhibition of HIV-1 reverse transcriptase by the novel broad-range DNA polymerase inhibitor N-{2-[4-(aminosulfonyl)phenyl]ethyl}-2-(2-thienyl)acetamide. *Biochemistry* **2008**, *47*, 490–502.
(17) Ahgren, C.; Backro, K.; Bell, F. W.; Cantrell, A. S.; Clemens, M.; Colacino, J. M.; Deeter, J. B.; Engelhardt, J. A.; Hogberg, M.; Jaskunas, S. R.; Johansson, N. G.; Jordan, C. L.; Kasher, J. S.; Kinnick, M. D.; Lind, P.; Lopez, C.; Morin, J. M., Jr.; Muesing, M. A.; Norren, R.; Oberg, B.; Paget, C. J.; Palkowitz, J. A.; Parrish, C. A.; Pranc, P.; Rippy, M. K.; Rydergard, C.; Sahlberg, C.; Swanson, S.; Ternansky, R. J.; Unge, T.; Vasileff, R. T.; Vrang, L.; West, S. J.; Zhang, H.; Zhou, X.-X. The PETT series, a new class of potent nonnucleoside inhibitors of human immunodeficiency virus type 1 reverse transcriptase. *Antimicrob. Agents Chemother.* **1995**, *39*, 1329–1335.
(18) Ren, J.; Diprose, J.; Warren, J.; Esnouf, R. M.; Bird, L. E.; Ikemizu, S.; Slater, M.; Milton, J.; Balzarini, J.; Stuart, D. I.; Stammers, D. K. Phenylethylthiazolylthiourea (PETT) non-nucleoside inhibitors of HIV-1 and HIV-2 reverse transcriptases. Structural and biochemical analyses. *J. Biol. Chem.* **2000**, *275*, 5633–5639.
(19) Merluzzi, V. J.; Hargrave, K. D.; Labadia, M.; Grozinger, K.; Skoog, M.; Wu, J. C.; Shih, C. K.; Eckner, K.; Hattox, S.; Adams, J.; Rosehthal, A. S.; Faanes, R.; Eckner, R. J.; Koup, R. A.; Sullivan, J. L. Inhibition of HIV-1 replication by a nonnucleoside reverse transcriptase inhibitor. *Science* **1990**, *250*, 1411–1413.
(20) Artico, M.; Di Santo, R.; Costi, R.; Novellino, E.; Greco, G.; Massa, S.; Tramontano, E.; Marongiu, M. E.; De Montis, A.; La Colla, P. Geometrically and conformationally restrained cinnamoyl compounds as inhibitors of HIV-1 integrase: Synthesis, biological evaluation, and molecular modeling. *J. Med. Chem.* **1998**, *41*, 3948–3960.
(21) Tramontano, E.; Esposito, F.; Badas, R.; Di Santo, R.; Costi, R.; La Colla, P. 6-[1-(4-Fluorophenyl)methyl-1H-pyrrol-2-yl)]-2,4-dioxo-5-hexenoic acid ethyl ester a novel diketo acid derivative which selectively inhibits the HIV-1 viral replication in cell culture and the ribonuclease H activity in vitro. *Antiviral Res.* **2005**, *65*, 117–124.
(22) Barreca, M. L.; Rao, A.; De Luca, L.; Iraci, N.; Monforte, A. M.; Maga, G.; De Clercq, E.; Pannecouque, C.; Balzarini, J.; Chimirri, A. Discovery of novel benzimidazolones as potent non-nucleoside reverse transcriptase inhibitors active against wild-type and mutant HIV-1 strains. *Bioorg. Med. Chem. Lett.* **2007**, *17*, 1956–1960.
(23) Balzarini, J.; Perez-Perez, M. J.; Velazquez, S.; San-Felix, A.; Camarasa, M. J.; De Clercq, E.; Karlsson, A. Suppression of the breakthrough of human immunodeficiency virus type 1 (HIV-1) in cell culture by thiocarboxanilide derivatives when used individually or in combination with other HIV-1-specific inhibitors (i.e., TSAO derivatives). *Proc. Natl. Acad. Sci. U.S.A.* **1995**, *92*, 5470–5474.
(24) Gadhachanda, V. R.; Wu, B.; Wang, Z.; Kuhen, K. L.; Caldwell, J.; Zondler, H.; Walter, H.; Havenhand, M.; He, Y. 4-Aminopyrimidines as novel HIV-1 inhibitors. *Bioorg. Med. Chem. Lett.* **2007**, *17*, 260–265.

(25) Hizi, A.; Herschhorn, A. Retroviral reverse transcriptases (other than those of HIV-1 and murine leukemia virus): A comparison of their molecular and biochemical properties. *Virus Res.* **2008**, *134*, 203–220.

(26) Barreiro, G.; Kim, J. T.; Guimaraes, C. R.; Bailey, C. M.; Domaoal, R. A.; Wang, L.; Anderson, K. S.; Jorgensen, W. L. From Docking False-Positive to Active Anti-HIV Agent. *J. Med. Chem.* **2007**, *50*, 5324–5329.

(27) Pelemans, H.; Esnouf, R. M.; Jonckheere, H.; De Clercq, E.; Balzarini, J. Mutational analysis of Tyr-318 within the non-nucleoside reverse transcriptase inhibitor binding pocket of human immunodeficiency virus type I reverse transcriptase. *J. Biol. Chem.* **1998**, *273*, 34234–34239.

(28) Balzarini, J.; Karlsson, A.; Vandamme, A. M.; Perez-Perez, M. J.; Zhang, H.; Vrang, L.; Oberg, B.; Backbro, K.; Unge, T.; San-Felix, A.; et al. Human immunodeficiency virus type 1 (HIV-1) strains selected for resistance against the HIV-1-specific [2′,5′-bis-O-(tert-butyldimethylsilyl)-3′-spiro-5″-(4″-amino-1″,2″-oxathiole-2″,2″-dioxide)]-β-D-pentofuranosyl (TSAO) nucleoside analogues retain sensitivity to HIV-1-specific nonnucleoside inhibitors. *Proc. Natl. Acad. Sci. U.S.A.* **1993**, *90*, 6952–6956.

(29) Ren, J.; Milton, J.; Weaver, K. L.; Short, S. A.; Stuart, D. I.; Stammers, D. K. Structural basis for the resilience of efavirenz (DMP-266) to drug resistance mutations in HIV-1 reverse transcriptase. *Structure* **2000**, *8*, 1089–1094.

(30) Halgren, T. A. MMFF VII. Characterization of MMFF94, MMFF94s and other widely available force fields for conformational energies and for intermolecular interaction energies and geometries. *J. Comput. Chem.* **1999**, *20*, 730–748.

(31) Jain, A. N. Surflex: Fully automatic flexible molecular docking using a molecular similarity-based search engine. *J. Med. Chem.* **2003**, *46*, 499–511.

(32) Sevilya, Z.; Loya, S.; Adir, N.; Hizi, A. The ribonuclease H activity of the reverse transcriptases of human immunodeficiency viruses type 1 and type 2 is modulated by residue 294 of the small subunit. *Nucleic Acids Res.* **2003**, *31*, 1481–1487.

(33) Hizi, A.; Tal, R.; Shaharabany, M.; Currens, M. J.; Boyd, M. R.; Hughes, S. H.; McMahon, J. B. Specific inhibition of the reverse transcriptase of human immunodeficiency virus type 1 and the chimeric enzymes of human immunodeficiency virus type 1 and type 2 by nonnucleoside inhibitors. *Antimicrob. Agents Chemother.* **1993**, *37*, 1037–1042.

(34) Hizi, A.; Tal, R.; Shaharabany, M.; Loya, S. Catalytic properties of the reverse transcriptases of human immunodeficiency viruses type 1 and type 2. *J. Biol. Chem.* **1991**, *266*, 6230–6239.

(35) Parniak, M. A.; Min, K. L.; Budihas, S. R.; Le Grice, S. F.; Beutler, J. A. A fluorescence-based high-throughput screening assay for inhibitors of human immunodeficiency virus-1 reverse transcriptase-associated ribonuclease H activity. *Anal. Biochem.* **2003**, *322*, 33–39.

(36) Loya, S.; Bakhanashvili, M.; Kashman, Y.; Hizi, A. Mechanism of inhibition of HIV reverse transcriptase by toxiusol, a novel general inhibitor of retroviral and cellular DNA polymerases. *Biochemistry* **1995**, *34*, 2260–2266.

(37) Loya, S.; Rudi, A.; Kashman, Y.; Hizi, A. Mode of inhibition of HIV-1 reverse transcriptase by polyacetylenetriol, a novel inhibitor of RNA- and DNA-directed DNA polymerases. *Biochem. J.* **2002**, *362*, 685–692.

(38) Roehm, N. W.; Rodgers, G. H.; Hatfield, S. M.; Glasebrook, A. L. An improved colorimetric assay for cell proliferation and viability utilizing the tetrazolium salt XTT. *J. Immunol. Methods* **1991**, *142*, 257–265.

(39) Naldini, L.; Blomer, U.; Gage, F. H.; Trono, D.; Verma, I. M. Efficient transfer, integration, and sustained long-term expression of the transgene in adult rat brains injected with a lentiviral vector. *Proc. Natl. Acad. Sci. U.S.A.* **1996**, *93*, 11382–11388.

JM800473D